Sinha *et al. Emerg. Contam. Environ. Health* **2025**, *1*, 6
DOI: 10.20517/eceh.2025.27

Emerging Contaminants and Environmental Health

Research Article

Open Access

Check for updates

Choline chloride-modified hydrochar from organic waste for the removal of PFOA from aqueous matrices: feasibility, isotherm, and kinetic studies

Sagarika Sinha, Byomkesh Mahanty, Subrata Hait

Department of Civil and Environmental Engineering, Indian Institute of Technology Patna, Bihar 801106, India.

Correspondence to: Dr. Subrata Hait, Department of Civil and Environmental Engineering, Indian Institute of Technology Patna, Bihar 801106, India. E-mail: shait@iitp.ac.in

How to cite this article: Sinha, S.; Mahanty, B.; Hait, S. Choline chloride-modified hydrochar from organic waste for the removal of PFOA from aqueous matrices: feasibility, isotherm, and kinetic studies. *Emerg. Contam. Environ. Health* **2025**, *1*, 6. https://dx.doi.org/10.20517/eceh.2025.27

Received: 30 Jun 2025 **First Decision:** 21 Aug 2025 **Revised:** 25 Sep 2025 **Accepted:** 16 Oct 2025 **Published:** 6 Nov 2025

Academic Editor: Daoji Li **Copy Editor:** Pei-Yun Wang **Production Editor:** Pei-Yun Wang

Abstract

This study investigated the feasibility of valorizing potato peel, a widely generated organic waste, through hydrothermal carbonization to produce hydrochar for the removal of perfluorooctanoic acid (PFOA), an emerging contaminant from aqueous matrices. Hydrochar was synthesized under four operating conditions, combining two temperatures (180 and 200 °C) with two reaction times (2 and 4 h). The hydrochar produced at 180 °C for 4 h exhibited the maximum specific surface area (28.055 m^2/g) and was selected for modification with 0.1 M choline chloride (ChCl) to enhance its adsorption performance. After modification, the specific surface area increased to 62.188 m^2/g, indicating an improved surface area. Batch adsorption experiments using 0.1 M ChCl-modified hydrochar (ChCl-HC) in the presence of 20 mM calcium chloride ($CaCl_2$) showed increased PFOA removal efficiency (95.4%) at 400 mg/L optimal adsorbent dose, attributed to Ca^{2+} induced bridging effect and electrostatic interactions. The adsorption isotherm model showed that the Langmuir model best fit the experimental data [the coefficient of determination (R^2) = 0.9976], followed by the Dubinin-Radushkevich (D-R), Temkin, and Freundlich models. The maximum monolayer adsorption capacity was calculated to be 72.621 mg/g, and the separation factor (0.030) indicated favorable adsorption. The calculated mean adsorption energy (1.35 kJ/mol) from the D-R model suggested physical adsorption. Kinetic analysis further showed that the data fit well with the pseudo-second order. Overall, three mechanisms were identified as responsible for PFOA adsorption on the 0.1 M ChCl-HC: electrostatic interaction, hydrogen bonding, and hydrophobic interaction. These findings

© The Author(s) 2025. **Open Access** This article is licensed under a Creative Commons Attribution 4.0 International License (https://creativecommons.org/licenses/by/4.0/), which permits unrestricted use, sharing, adaptation, distribution and reproduction in any medium or format, for any purpose, even commercially, as long as you give appropriate credit to the original author(s) and the source, provide a link to the Creative Commons license, and indicate if changes were made.

highlight that ChCl-HC, combined with $CaCl_2$ serving as a bridging agent, offers a sustainable and efficient solution for PFOA removal. Overall, this approach offers a promising solution for the valorization of organic waste into hydrochar, with potential application in the removal of PFOA, an emerging contaminant, from aqueous matrices.

Keywords: Organic waste, hydrothermal carbonization, hydrochar, perfluorooctanoic acid, choline chloride, calcium chloride

INTRODUCTION

The management of organic waste has become a growing global concern driven by the urgent need for sustainable and environmentally responsible solutions. Organic waste, comprising biodegradable materials derived from plant and animal sources, constitutes a significant portion of the global waste stream. It originates from various sources including municipal solid waste, agricultural residues, and various commercial and industrial activities. Improper handling and disposal of such waste contribute significantly to environmental degradation and greenhouse gas (GHG) emissions[1,2]. Annually, an estimated 11.2 billion tons of solid waste are collected worldwide, with the subsequent decomposition of its organic components contributing approximately 5% of global GHG emissions[3]. In this context, organic waste valorization has gained attention as a sustainable alternative to conventional waste disposal methods. This approach focuses on the conversion of organic waste into valuable products, thereby promoting resource recovery and reducing the environmental impact. One specific example of underutilized organic waste is potato peel waste. Potato processing generates a significant amount of peel waste, typically ranging from 15% to 40% of the potato's initial weight. Projections suggest that global potato peel waste production could reach approximately 8,000 kilotons by 2030. This substantial waste stream is estimated to contribute approximately 5 million tons of CO_2-equivalent GHG emissions[4,5].

To address this environmental challenge, hydrothermal carbonization (HTC) has emerged as a promising thermochemical technique for the valorization of organic waste, including potato peel waste, into value-added products, particularly hydrochar (HC), a carbon-rich and porous solid material. One of the key environmental benefits of HTC is its high efficiency in carbon sequestration, as a significant portion of the carbon from the original organic waste feedstock is retained in the resulting hydrochar, thereby contributing to climate change mitigation[6]. The HTC process is generally performed in a sealed hydrothermal autoclave, typically at a temperature between 150-250 °C, under autogenous pressure, transforming the organic waste into HC[7]. It is a solid carbonaceous material produced under subcritical water conditions through a combination of reactions, including hydrolysis, dehydration, decarboxylation, condensation, polymerization, and aromatization[8,9]. HC is a porous carbonaceous material enriched with oxygen-containing groups such as hydroxyl, carboxyl, and carbonyl groups. These functional groups enhance its surface reactivity, facilitating the effective adsorption of a wide range of pollutants. This makes it a promising precursor for the development of advanced adsorbent materials. Elevated HTC temperature and extended reaction time intensify carbonization, leading to the development of micropores and mesopores that enhance surface area and pore volume. At higher temperatures, accelerated hydrolysis and dehydration release volatile compounds, generating voids and enlarging pore size, while greater water reactivity promotes hydrolysis and condensation[10]. Fang *et al.* observed a better specific surface area of the hydrochar synthesized at temperature below 200 °C[11]. However, prolonged reaction time produces hydrochar that resembles lignite coal, showing reduced oxygen and hydrogen content due to extensive dehydration, decarboxylation, and aromatization. For adsorption applications, hydrochar synthesized under optimal conditions of temperature and reaction time is preferable as it retains higher oxygen content and more favorable surface functionalities[12-14]. In addition, its favorable physicochemical properties underscore its potential as a cost-effective and sustainable adsorbent for the removal of both organic and inorganic

contaminants from aqueous matrices[6,15]. Furthermore, its surface characteristics can be modified to enhance adsorption performance, broadening its applicability in environmental remediation[16].

HC has been increasingly studied for its effectiveness in removing emerging contaminants such as pharmaceuticals and personal care products, endocrine-disrupting compounds, per- and polyfluoroalkyl substances (PFAS), *etc*. PFAS are a group of synthetic chemicals that have become a significant environmental concern due to their persistence, resistance to degradation, and potential adverse effects on human health, hence called "forever chemicals"[17]. Perfluorooctanoic acid (PFOA), a long-chain PFAS compound, has exceptional environmental persistence, primarily attributed to the strength of its carbon-fluorine bonds, which contribute to extreme stability, inertness, and low surface energy[18]. Its non-polar fluorinated tail renders it both hydrophobic and lipophobic in nature, while its carboxyl functional polar head group is hydrophilic and interacts readily with water, showing an amphiphilic character. It has been widely employed in various industrial and consumer products such as non-stick cookware, stain- and water-resistant textiles, food packaging, and firefighting foam because of its stability and physicochemical properties[19]. PFOA under typical environmental pH conditions primarily exists in its anionic form and is highly soluble in water. However, ecological release of PFOA can occur throughout its life cycle, encompassing production, manufacturing, use, and disposal stages[20-23]. Despite its long-standing use, concerns over PFOA's toxicity emerged in the early 2000s, leading the United States Environmental Protection Agency (USEPA) to classify PFOA as a potential carcinogen in 2009[24]. In 2025, the maximum contaminant levels (MCLs) for PFOA in drinking water given by USEPA were 4.0 ng/L[25]. Consequently, removing PFOA from contaminated water has become a pressing research focus.

Conventional PFOA removal methods are constrained by high costs, incomplete removal, and the generation of secondary waste, emphasizing the need for more efficient and sustainable solutions. Adsorption has emerged as a promising and cost-effective strategy, with growing research focused on its effectiveness in removing the PFOA compound from water systems[26]. Although numerous studies have investigated the adsorption of PFOA using activated carbon, biochar, and other carbonaceous materials, there is limited research available on the use of HC as an adsorbent. In a study conducted by Chen *et al.*, activated HC derived from food waste was investigated for the adsorption of PFAS compounds, including PFOA[27]. In the present study, we studied the potential role of choline chloride (ChCl) modified potato peel waste-based HC, in combination with calcium chloride ($CaCl_2$) as a bridging agent, for the removal of PFOA from aqueous matrices. ChCl, a quaternary ammonium salt that is low-cost, non-toxic, biodegradable, and biocompatible, can improve the surface functionality of pristine HC by introducing additional active sites[28,29]. In parallel, the presence of Ca^{2+} ions facilitates divalent cation bridging between the adsorbent surface and PFOA molecules, thereby enhancing the overall adsorption performance[30,31].

In these contexts, the porous HC was prepared through the HTC process and subsequently modified with ChCl for its application in the PFOA removal from aqueous solutions. The objective of the study was to prepare and characterize HC derived from potato peel waste, and based on its maximum specific surface area, further modify it using ChCl through physical adsorption[32] of varying concentrations. The PFOA removal efficiencies of both pristine HC and modified HCs were evaluated in the presence and absence of $CaCl_2$, used as a bridging agent. Adsorption isotherm and kinetic studies were conducted on selected ChCl-HC to assess its adsorption behaviour. Overall, the study aimed to enhance the removal efficiency of HC and contribute to the development of a sustainable and efficient solution for the removal of PFOA from aqueous solution.

EXPERIMENTAL

Feedstocks and chemicals

Potato peel waste used for hydrochar production was collected from the mess of Asima Hostel at the Indian Institute of Technology, Patna, Bihar, India. After collection, it was thoroughly washed with tap water, followed by deionized (DI) water to remove surface impurities. It was sun-dried for several days, and the dried peels were ground and sieved to obtain a size less than 1 mm. Then it was stored in a sealed zip-lock bag to prevent it from moisture. The grinding of potato peel waste was conducted to increase the uniformity.

Choline chloride (C_5H_{14}·ClNO, ≥ 98 %) of Loba Chemie Pvt. Ltd., calcium chloride ($CaCl_2$ ≥ 98%), PFOA (CAS number: 335-67-1, $C_8HF_{15}O_2$, 95%), high performance liquid chromatography (HPLC) grade water, HPLC grade acetonitrile (CH_3CN), and di-sodium hydrogen phosphate (Na_2HPO_4, ≥ 99%) were purchased from Merck, India. All the reagents and chemicals were of analytical grade and used without further purification in the experiments. Milli-Q water filtered through a 0.22 μm filter paper was utilized to prepare all experimental solutions employed in the study.

Preparation of hydrochar

HTC of potato peel waste was carried out using a 100 mL Teflon-lined stainless steel hydrothermal autoclave reactor. The experiments were performed under autogenous pressure at two different temperatures (180 and 200 °C) and two different reaction times (2 and 4 h). A 1:10 solid-to-liquid ratio of potato peel waste to DI water was used. The mixture was placed in the reaction vessel, which was then tightly sealed within the reactor. After the completion of the reaction time, the reactor was allowed to cool naturally at ambient room temperature. After cooling, the solid-liquid mixture was separated using a 0.22 μm membrane filter in a vacuum filtration unit, and subsequently washed thoroughly with DI water to remove any adhering soluble impurities. Finally, the HC dried in an oven at 60 °C for 24 h to remove residual moisture, and the obtained dry sample was stored in an airtight container for further characterization and use.

Modification of hydrochar

The HC obtained at 180 °C for 4 h (further referred to as pristine HC) was subjected to surface modification using two different concentrations, 0.05 and 0.1 M, of ChCl solution. For the modification process, the pristine HC was mixed with the respective ChCl solution and stirred continuously for 3 h at 70 °C to promote better surface interaction and functionalization. Following the reaction, the modified HC was allowed to cool to room temperature. It was then separated and thoroughly washed with DI water to eliminate the unbound ChCl. The resulting ChCl-HC was subsequently dried overnight at 60 °C. The dried ChCl-HC was designated as 0.05 M ChCl-HC and 0.1 M ChCl-HC, respectively, and stored in airtight containers for subsequent characterization and adsorption experiments.

Hydrochar characterizations

Elemental compositions of pristine HCs and modified hydrochar were determined using the CHNS analyzer Leco TruSpec Micro instrument. The Brunauer–Emmett–Teller (BET) specific surface area and porosity were calculated from N_2 adsorption–desorption isotherm curves using a Quantachrome Autosorb iQ2 analyzer. Thermogravimetric analysis (TGA) and derivative thermogravimetric analysis (DTG) were determined in Discovery series, TA SDT650. An X-ray diffractometer (XRD) (Rigaku X-ray diffractometer) using Cu-K radiation (λ = 1.5418 Å) in the 2θ range from 10° to 90° was employed to examine the crystal structures of the prepared materials. Fourier-transform infrared (FTIR) analysis was conducted using a Bruker Vertex V80 spectrometer in attenuated total reflectance (ATR) mode to determine the functional groups present on the surface. The morphology was characterized by using field emission scanning electron

microscopy (FESEM, Hitachi S-4800) by gold coating on the hydrochar powder through direct current (DC) sputtering technique. Zeta (ζ) potential values were recorded to determine the point of zero charge (pH_{ZPC}) of the adsorbent over a pH range of 2-12 (Anton Paar, Litesizer 500 particle analyzer).

Batch adsorption experiments

The preliminary experiments were carried out using prepared adsorbents, namely, pristine HC, 0.05 M ChCl-HC, and 0.1 M ChCl-HC, with and without 20 mM of $CaCl_2$ as a bridging agent, to evaluate their effectiveness in removing PFOA from aqueous solution. Among these, the adsorbent exhibiting the maximum removal efficiency was selected for further study. Based on the initial studies, 0.1 M ChCl-HC demonstrated better adsorption performance and was thus chosen for subsequent batch adsorption studies. The batch experiments were performed in 125 mL polypropylene flasks, each containing 50 mL of PFOA solution with an initial concentration of 20 mg/L (pH: ~4.4). The dose of adsorbent varied from 20 to 600 mg/L, along with 20 mM of $CaCl_2$ as a bridging agent. The flasks were agitated at 250 rpm in a temperature-controlled environment maintained at 298 K for a contact time of 120 min. Upon completion of the adsorption process, 2 mL of aliquots were acquired from each flask, filtered through a 0.22 μm syringe filter to remove suspended particles, and the filtrates were subsequently analyzed using HPLC to measure the concentration of remaining PFOA in the aqueous phase.

The equilibrium adsorption capacity of the PFOA was calculated according to[31]

$$q_e = \left(\frac{C_0 - C_e}{m}\right) \times V \quad (1)$$

where q_e (mg/g) represents the amount of PFOA adsorbed per unit mass of the adsorbent, while C_0 (mg/L) and C_e (mg/L) stand for the initial and equilibrium concentrations of the PFOA in solution, respectively. V denotes the volume of the PFOA solution (L), and m indicates the mass of adsorbent (g).

The removal percentage is calculated as follows[31]:

$$R\ (\%) = \left(\frac{C_0 - C_e}{C_0}\right) \times 100 \quad (2)$$

where R (%) is the PFOA removal percentage, while C_0 (mg/L) and C_e (mg/L) stand for the initial and equilibrium concentrations of the PFOA in solution, respectively.

Adsorption isotherms

Adsorption isotherm models were applied to the experimental data obtained from the dose variation study, conducted over a concentration range of 20 to 600 mg/L using 0.1 M ChCl-HC as the adsorbent. The adsorption behavior was evaluated using four widely accepted isotherm models: Langmuir, Freundlich, Temkin, and Dubinin-Radushkevich (D-R).

The linear forms of these models, along with their respective parameters and descriptions, are summarized in Table 1. The Langmuir isotherm, initially proposed to describe gas-phase adsorption onto solid surfaces, has been extensively applied as a theoretical model to characterize adsorption processes across a wide range of adsorbent materials. The Langmuir isotherm is based on four fundamental assumptions: (i) adsorption occurs as a monolayer, with adsorbate molecules forming a single molecular layer on the adsorbent surface; (ii) all adsorption sites are homogeneous and possess identical energetic characteristics; (iii) the adsorption energy remains constant across all active sites; and (iv) there are no lateral interactions between adjacent adsorbed molecules[33]. The Freundlich isotherm is an empirical model that describes adsorption on

Table 1. Equations of isotherm models

Isotherm models	Equations	Description
Langmuir[34]	$\frac{C_e}{q_e}=\frac{C_e}{q_{max}}+\frac{1}{K_L q_{max}}$ $R_L=\frac{1}{1+(C_0\times K_L)}$	C_e: Equilibrium concentration of adsorbate (mg/L) q_e: Adsorption capacity adsorbed at equilibrium (mg/g) q_{max}: Maximum adsorption capacity (mg/g) K_L: Langmuir adsorption constant (L/mg) R_L: separation factor
Freundlich[34]	$\log_e q_e=\log K_f+\frac{1}{n}\log C_e$	K_f: Freundlich constant [(mg/g) (L/mg)$^{1/n}$] n: Adsorption intensity constant R: Universal gas constant (8.314 J/mol K) T: Temperature (K)
Temkin[34]	$q_e=B_T \ln A+B_T \ln C_e$	B_T: Temkin isotherm constant related to heat of adsorption (J/mol) A: Equilibrium binding constant (L/g)
D-R[34]	$\ln q_e=\ln q_{max}-K\cdot\varepsilon^2$ $\varepsilon=RT\ln\left(1+\frac{1}{C_e}\right)$ $E=\frac{1}{\sqrt{2K}}$	K: D-R constant, related to mean adsorption energy (mol^2/kJ^2) ε: Polanyi potential E: Mean free energy (kJ/mol)

D-R: Dubinin-Radushkevich.

heterogeneous surfaces, accommodating both monolayer (chemisorption) and multilayer (physisorption) adsorption. Unlike the Langmuir isotherm, it accounts for non-uniform surface energies and varying affinities across adsorption sites. The model assumes an exponential decay in adsorption energy distribution, making it suitable for systems with heterogeneous surfaces and multilayer adsorption behavior[33]. The Temkin isotherm model accounts for multilayer adsorbent–adsorbate interactions by assuming that the adsorption energy decreases linearly with increasing surface coverage. It describes adsorption behavior over a moderate concentration range, neglecting extremely low and high concentrations[34]. The D-R isotherm is a semi-empirical model that describes adsorption based on a pore-filling mechanism rather than surface coverage, making it broader than the Langmuir and Freundlich models. It also enables the estimation of mean adsorption energy, providing insights into the adsorption mechanism[33,34].

Adsorption kinetics

Adsorption kinetics were examined at an initial PFOA concentration of 20 mg/L and a fixed adsorbent dose of 400 mg/L, with contact times of 5, 10, 20, 30, 60, 120, 180, and 240 min. The experimental data were fitted to pseudo-first-order, pseudo-second-order, Elovich, and intra-particle diffusion models, with their equations and descriptions provided in Table 2.

Influence of humic acid, bridging ion, and reusability

The effect of humic acid on PFOA adsorption was evaluated over a concentration range of 10-50 mg/L. In addition, $CaCl_2$ was examined at concentrations of 5-50 mM to investigate the bridging effect of varying $CaCl_2$ concentrations on PFOA adsorption. Adsorbent regeneration was carried out using a 50% ethanol-water mixture as the desorption reagent[35]. Briefly, after each cycle, the spent adsorbent was treated with a 50% ethanol-water solution under agitation at 200 rpm for 12 h at room temperature. Upon completion, the adsorbent was recovered through centrifugation and thoroughly rinsed with DI water and then dried for subsequent reuse. All the experiments were performed in triplicate to ensure the reliability of the results.

RESULTS AND DISCUSSION

Characterizations of adsorbents

Elemental compositions and BET analysis

The elemental compositions of HCs synthesized at 180 °C (2 and 4 h) and 200 °C (2 and 4 h), along with the 0.1 M ChCl-HC, are summarized in Supplementary Table 1. The carbon content of the HCs increased progressively with rising temperature and reaction time, from 49.916% at 180 °C for 2 h to 60.640% at 200 °C for 4 h, attributed to dehydration and decarboxylation reactions that eliminate oxygenated groups

Table 2. Kinetic model equation and parameters

Kinetic models	Equations	Description
Pseudo-first-order model[14]	$\ln(q_e-q_t)=\ln q_e-k_1 t$	q_t (mg/g): Adsorption capacities at time t q_e (mg/g): Adsorption capacities at equilibrium time k_1 (min^{-1}): Pseudo-first-order rate constant k_2 (g/mg/min): Pseudo-second-order rate constant α (mg/g/min): Rate of adsorption constants β (g/mg): Rate of desorption constants k_d ($mg/g/min^{0.5}$): Rate constant C (mg/g): Intercept
Pseudo-second-order model[14]	$\frac{t}{q_t}=\frac{1}{k_2 q_e^2}+\frac{t}{q_e}$	
Elovich model[68]	$q_t=\beta \ln(\alpha\beta)+\beta \ln t$	
Intra-particle diffusion[34]	$q_t=k_d \times t^{0.5}+C$	

during HTC. Correspondingly, oxygen contents declined significantly from 37.07% to 26.78%, suggesting the formation of a more aromatic and hydrophobic carbon matrix. Furthermore, the elemental analysis revealed that the 0.1 M ChCl-HC exhibits a slight increase in carbon (55.106%) and hydrogen (6.057%) contents compared to the pristine HC (180 °C and 4 h). Also, an increase in nitrogen content from 5.711% to 5.845% depicts the successful doping of nitrogen from choline chloride.

To further investigate the textural characteristics of the HCs, N_2 adsorption-desorption isotherms were analyzed using the BET method. Among all the synthesized HCs [Supplementary Table 1], those prepared at 180 °C for 4 h (pristine HC) exhibited the maximum BET specific surface area of 28.055 m^2/g and were therefore selected for surface modification. Upon modification with 0.1 M ChCl, a notable improvement in surface characteristics was observed, with the BET specific surface area increasing to 62.188 m^2/g. The N_2 adsorption-desorption isotherms of both the pristine HC and 0.1 M ChCl-HC are presented in Figure 1A and B[14]. The isotherm for both the materials corresponds to type IV with H3 hysteresis loops, indicative of mesoporous structure. The pore size distribution of pristine HC and 0.1 M ChCl-HC was analyzed using the non-local density functional theory (NLDFT) approach [Figure 1C and D]. Notably, both pristine HC and 0.1 M ChCl-HC exhibited an average pore width of 27.690 Å (2.769 nm), further confirming their mesoporosity[36]. The size of PFOA is approximately 1.13 nm in length, and the mesoporous hydrochar is sufficiently large to allow unhindered entry and rapid diffusion of PFOA molecules, along with a greater capacity for PFOA[37]. The pore volume increased from 0.040 to 0.072 cc/g after the modification with ChCl, indicating a significant improvement in the textural properties of the 0.1 M ChCl-HC.

TGA analysis

The thermal behavior of pristine HC and 0.1 M ChCl-HC was investigated using TGA. The TGA and DTG graphs of pristine HC and 0.1 M ChCl-HC are shown in Supplementary Figure 1A and B. The TGA graph [Supplementary Figure 1A] of both pristine and 0.1 M ChCl-HC exhibit three distinct weight loss regions: an initial minor loss below 110 °C correspond to moisture, second stage between 200-450 °C primarily due to the release of volatile matters and partial decomposition of hemicellulose and cellulose, and the last stage leads to complete thermal degradation of hemicellulose, cellulose, and lignin and more thermally stable aromatic and carbonaceous structures. The pristine HC shows slightly greater weight loss in the 200-450 °C region compared to 0.1 M ChCl-HC, indicating the choline chloride modification may enhance thermal stability by promoting the formation of more thermally resistant structures[38].

The DTG graph [Supplementary Figure 1B] further clarifies the decomposition behavior, where both samples exhibit a major degradation peak at approximately 353 °C. Notably, the intensity and sharpness of the peak were slightly reduced in the 0.1 M ChCl-HC, suggesting a more gradual thermal decomposition process. This could be attributed to the incorporation of choline chloride, which might influence the pyrolytic pathways and decomposition kinetics by altering the surface chemistry and functional groups of the HC matrix[39,40].

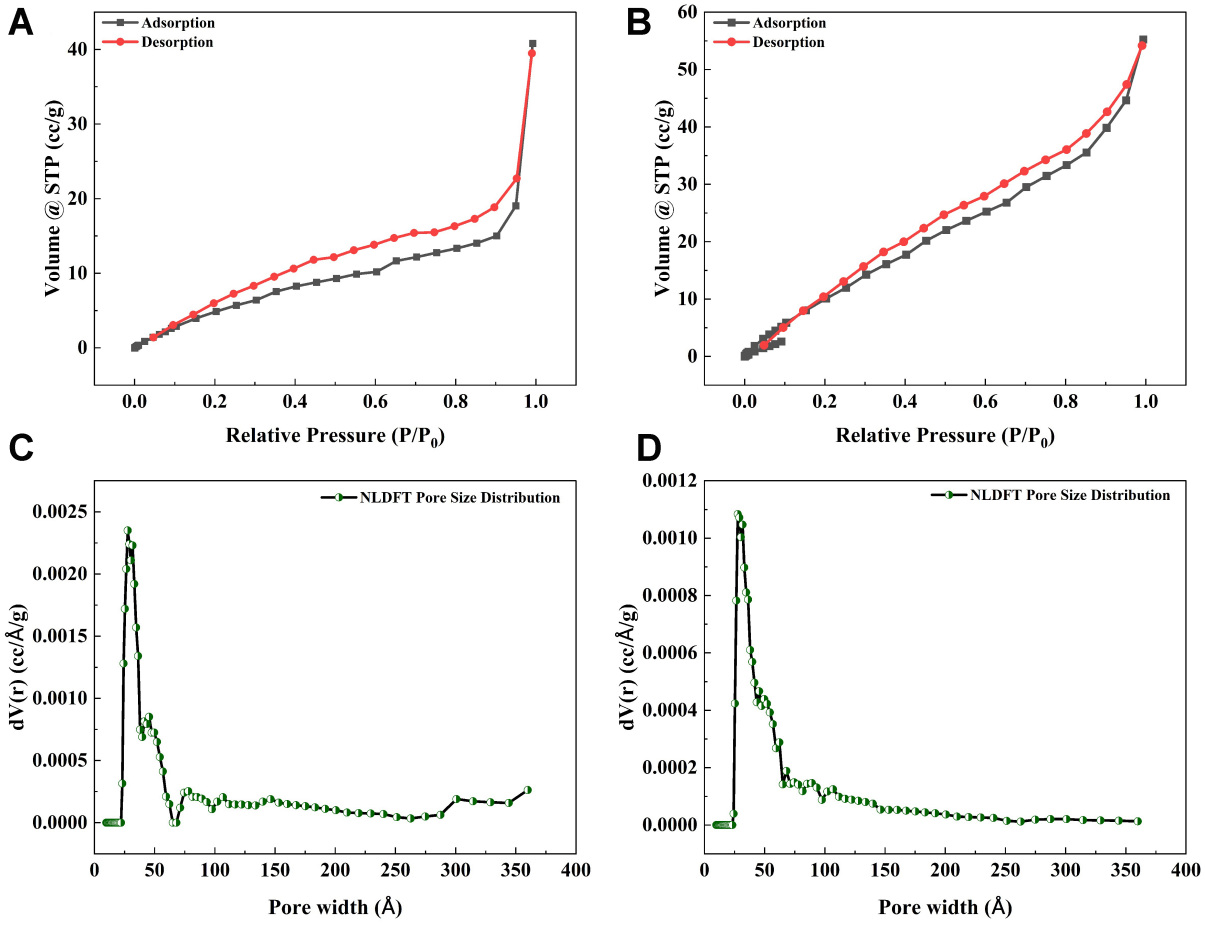


Figure 1. (A and B) BET analysis and (C and D) pore size distribution of pristine HC and 0.1 M ChCl-HC. BET: Brunauer–Emmett–Teller; ChCl-HC: ChCl-modified hydrochar.

X-ray diffraction analysis

To analyze the crystalline structure of pristine HC and 0.1 M ChCl-HC, powder X-ray diffraction (p-XRD) measurements were carried out, as shown in Supplementary Figure 2A. The XRD pattern of pristine HC reveals a distinct peak at 15° and a broad peak around 21.5°. Upon modification with choline chloride, 0.1 M ChCl-HC exhibits more defined and slightly intensified diffraction peaks at positions similar to those observed in pristine HC. The presence of a broad peak at around 21.5 is typically attributed to the (002) plane of amorphous and poorly crystalline structure[41].

pH_{zpc} analysis

The pH_{zpc} is a key parameter that defines the surface charge characteristics of an adsorbent. For 0.1 M ChCl-HC, the pH_{zpc} was determined across the pH range of 2-12 and found to be 4.9, indicating that the adsorbent surface was positively charged below pH 4.9 and negatively charged above it [Supplementary Figure 2B].

FESEM analysis

The morphological features of pristine HC and 0.1 M ChCl-HC were revealed through FESEM analysis, as presented in Supplementary Figure 2C and D. The FESEM image of pristine hydrochar [Supplementary Figure 2C] reveals compact vesicular and spherical particles, which appear clustered due to dehydration and aromatization reactions during the HTC process[42,43]. In contrast, the morphology of the 0.1 M ChCl-HC

[Supplementary Figure 2D] reveals a more fragmented and irregular morphology featuring increased textural roughness, disordered cavities, and exposed edges, likely due to the interaction between the ChCl and the hydrochar[44]. This enhanced structural complexity arises from the chemical action of ChCl, which interacts with the hydrochar matrix, promoting the development of new adsorption sites and pores.

FTIR analysis

The presence of functional groups in the hydrochars [Supplementary Figure 3] and 0.1 M ChCl-HC (before and after PFOA adsorption) [Figure 2A] was investigated using FTIR spectroscopy. In the raw hydrochars, the broad peak in the range of 3,492 to 3,170 cm^{-1} corresponds to hydroxyl stretching vibrations, whereas the peak in the range of 1,560 to 1,697 cm^{-1} is attributed to the C=O group; both showed a decrease in peak intensity and a shift to larger wavenumber due to decarboxylation and dehydration reaction. Apart from that, the decrease in the intensity of O–H and C=O peaks also suggests an increase in the hydrophobic nature of hydrochars[41,45]. The other characteristic peaks at 2,925-2,850 and 781-667 cm^{-1} correspond to C–H stretching vibrations and aromatic out-of-plane bending, respectively[45,46]. The peaks at 1,415 and 1,312 cm^{-1}, attributed to C=C stretching in aromatic groups, are evident in both the potato peels and the hydrochar, which diminishes with increased temperature, suggesting the presence of lignin fragments in the hydrochar[46]. The broad band observed between 1,000 and 1,170 cm^{-1}, which splits into multiple distinct bands, is associated with the deformation of C–O bonds and the stretching of C–C bonds from the residual cellulose and hemicellulose in the cell walls. These bands become less prominent as the temperature increases[46,47]. Upon modification of pristine HC with choline chloride [Figure 2A], the 0.1 M ChCl-HC exhibits a peak at 1,031 cm^{-1} corresponding to the symmetric stretching vibration of $C–N^+$, along with peaks at 718 and 674 cm^{-1} attributed to the asymmetric stretching vibrations of C–N, confirming the successful modification of hydrochar with ChCl[48,49].

Furthermore, to confirm PFOA adsorption onto 0.1 M ChCl-HC and better understand the underlying process, the FTIR spectrum of 0.1 M ChCl-HC after adsorption was analyzed, as shown in Figure 2A. In the FTIR spectrum of 0.1 M ChCl-HC after adsorption, new peaks emerged, which confirmed the successful adsorption of PFOA onto the surface of the developed adsorbent. After adsorption, the symmetric and asymmetric stretching vibration peaks of COO^- were observed at 1,475 and 1,709 cm^{-1}, respectively, in 0.1 M ChCl-HC, showing a blue shift compared to pristine PFOA [Figure 2A and B]. These changes might have been caused by the electrostatic interaction between PFOA and the adsorbent. The hydroxyl stretching vibration peak observed at 3,725 cm^{-1} exhibited a noticeable blue shift after adsorption, suggesting the involvement of hydrogen bonding in the removal of PFOA. Furthermore, the new peak at 1,287 cm^{-1} corresponds to the vibrations of the C-F on the 0.1 M ChCl-HC after adsorption of PFOA[50]. Overall, the observed spectral changes, including peak shifts and new peak formation, confirm the interaction between PFOA and 0.1 M ChCl-HC.

PFOA adsorption behaviors

Feasibility study

The feasibility study was conducted to assess the PFOA removal efficiency and adsorption capacity of pristine HC and ChCl-modified hydrochars, aiming to identify the adsorbent and conditions that yield the highest removal efficiency. The pristine HC exhibited a removal efficiency of 10%, whereas 0.05 M and 0.1 M ChCl-HC showed increased efficiencies of 32.15% and 35.65%, respectively [Figure 3A]. Pristine HC and PFOA are both anionic in nature, which likely resulted in electrostatic repulsion and hindered the effective removal of PFOA. Surface modification with ChCl introduced functional groups that likely reduced this repulsion, leading to improved removal performance. However, the overall enhancement in removal efficiency remained modest, indicating that while ChCl modification contributes positively, it may not be sufficient alone to achieve high PFOA removal efficiency.

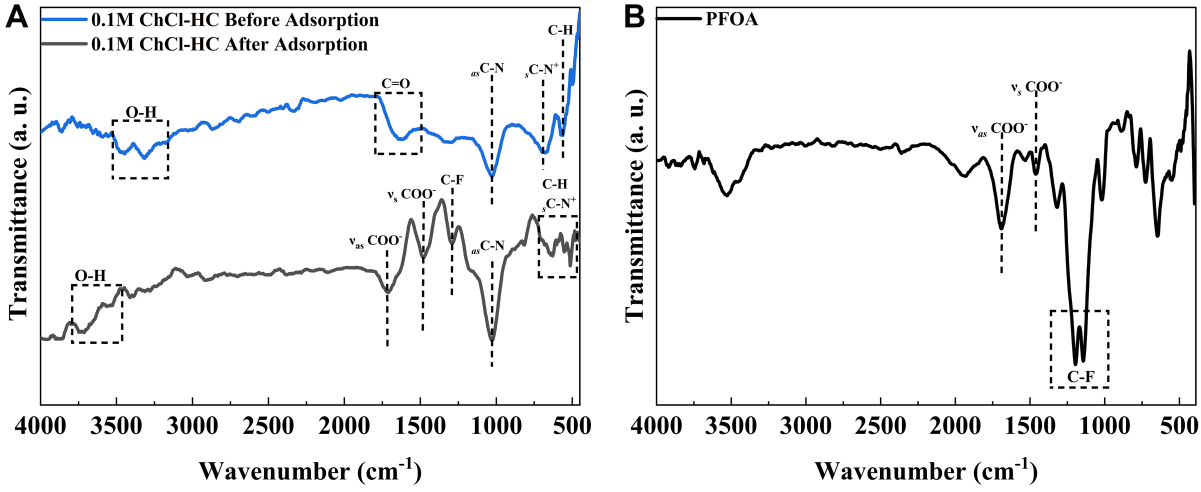


Figure 2. FTIR spectrum of 0.1 M ChCl-HC before and after adsorption of (A) PFOA and (B) pristine PFOA. FTIR: Fourier-transform infrared; ChCl-HC: ChCl-modified hydrochar; PFOA: perfluorooctanoic acid.

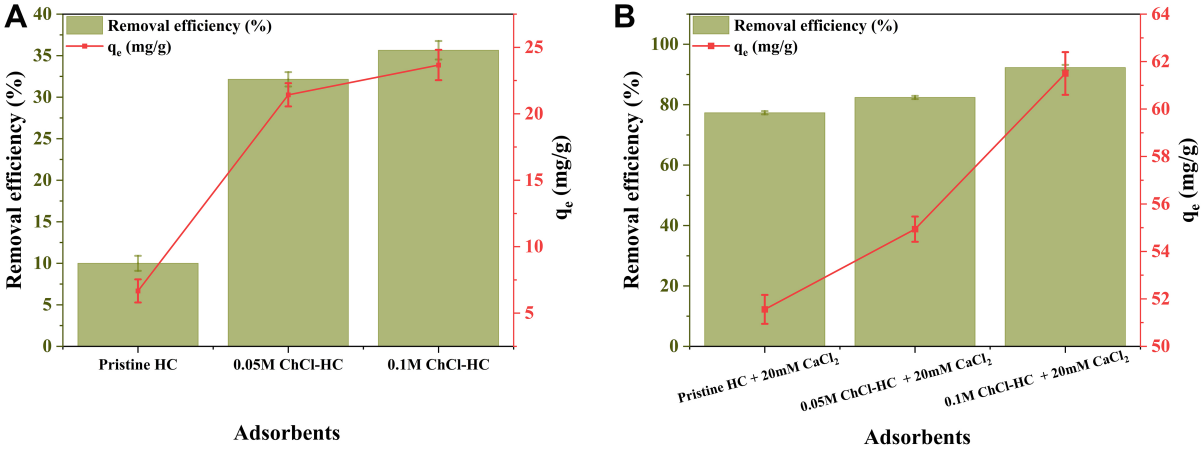


Figure 3. Removal efficiency and adsorption capacity of Pristine HC, 0.05 M ChCl-HC, and 0.1 M ChCl-HC (A) without $CaCl_2$ and (B) with $CaCl_2$ (Experimental conditions: PFOA concentration: 20 mg/L, Adsorbent dose: 300 mg/L, $CaCl_2$: 20 mM, Temperature: 298 K, and RPM: 250). ChCl-HC: ChCl-modified hydrochar; PFOA: perfluorooctanoic acid; RPM: revolutions per minute.

To further enhance the removal efficiency, a bridging agent, $CaCl_2$ of concentration 20 mM, was introduced into the adsorption experiment to facilitate the bridging effect between modified hydrochar and PFOA. The maximum removal efficiency (92.3%) and adsorption capacity (61.5 mg/g) were achieved using 0.1 M ChCl-HC in the presence of 20 mM $CaCl_2$ [Figure 3B]. The presence of Ca^{2+} ions enhanced the adsorption performance through a divalent cation bridging effect. Specifically, Ca^{2+} ions facilitated electrostatic interactions by bridging the negatively charged functional groups of hydrochar and the carboxylate head of PFOA[30,51].

Effect of adsorbent dosage on PFOA adsorption

A dose variation study was conducted to explore the influence of adsorbent quantity on PFOA removal, using 0.1 M ChCl-HC based on its superior performance. As shown in Figure 4, increasing the adsorbent dose from 20 to 600 mg/L resulted in a substantial rise in removal efficiency, reaching a maximum of 95.4%, likely due to the increased number of accessible adsorption sites. With an increase in dose to 600 mg/L, the

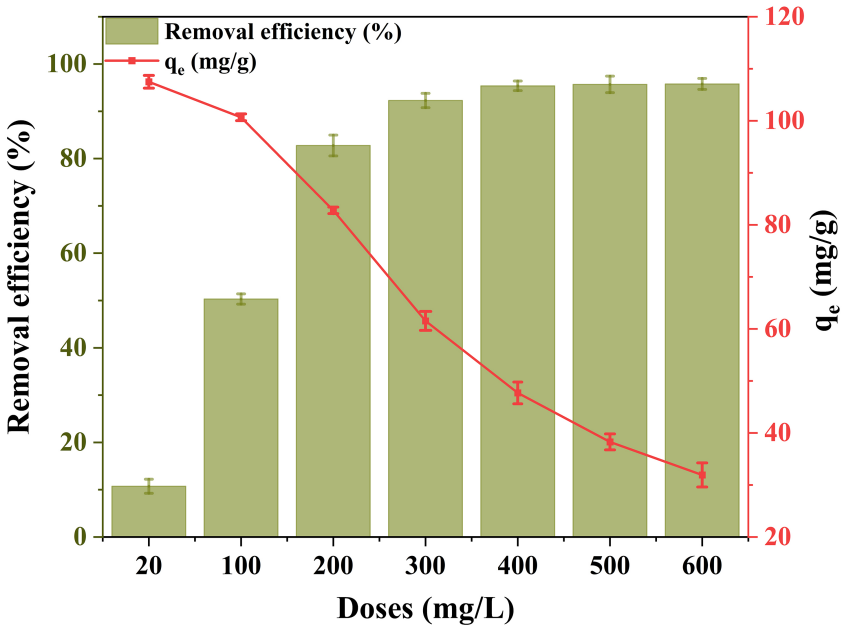


Figure 4. Effect of adsorbent dose on the removal of PFOA using 0.1 M ChCl-HC with 20 mM $CaCl_2$ (Experimental conditions: PFOA concentration: 20 mg/L, Adsorbent dose: 20-600 mg/L, $CaCl_2$: 20 mM, Temperature: 298 K, and RPM: 250). PFOA: Perfluorooctanoic acid; ChCl-HC: ChCl-modified hydrochar; RPM: revolutions per minute.

adsorption capacity declined to 31.9 mg/g, while the highest value of 107.5 mg/g was recorded at the lowest dose, likely because more active sites remained unoccupied during the adsorption process. The removal efficiency of PFOA remained largely unchanged and reached saturation beyond a 0.1 M ChCl-HC dose of 400 mg/L, which was therefore considered the optimal dose.

Adsorption isotherms

The adsorption isotherms analysis plays a crucial role in elucidating the underlying adsorption behavior of PFOA onto 0.1 M ChCl-HC. For understanding the dose-dependent adsorption behavior, four adsorption isotherm modeling techniques were applied: Langmuir [Figure 5A], Freundlich [Figure 5B], Temkin [Figure 5C], and D-R isotherm [Figure 5D]. Among these, the Langmuir isotherm exhibited the best fit model in the study with coefficient of determination (R^2) = 0.9979, followed by Temkin (R^2 = 0.9449), D-R (R^2 = 0.9447), and Freundlich (R^2 = 0.9383). Langmuir isotherm model, which provided the best fit, suggests the monolayer adsorption of PFOA on the homogeneous surface of 0.1M ChCl-HC[52]. The Langmuir constant (K_L) was calculated as 1.616, while the corresponding separation factor (R_L) was 0.030. The R_L value, lying between 0 and 1, confirms the favorable and spontaneous nature of the adsorption process[31,53]. Furthermore, the 1/n value (0.348) obtained from the Freundlich isotherm, being less than 1, indicates that the adsorption process is favorable[54]. The Temkin adsorption isotherm constant, related to the heat of adsorption (b_t) value, is greater than zero [Table 3], indicating the exothermic adsorption process[54]. In the D-R isotherm, the estimated mean free energy (E = 1.354 kJ/mol), which is below 8 kJ/mol, confirms that the adsorption process proceeds predominantly through a physical process[55]. Consequently, the isotherm analysis confirms that the adsorption of PFOA onto 0.1 M ChCl-HC is monolayer, favorable, and supports the physical adsorption.

Adsorption kinetics

Kinetic analysis of PFOA adsorption was performed using linear pseudo-first-order [Figure 6A], pseudo-

Table 3. Isotherm model parameters for PFOA adsorption onto 0.1 M ChCl-HC

Isotherm models	Parameters	Values
Langmuir	q_{max} (mg/g)	72.621
	K_L (L/mg)	1.616
	R^2	0.9979
Freundlich	K_f [(mg/g) (L/mg)$^{1/n}$]	44.530
	n	2.869
	R^2	0.9383
Temkin	A (L/mg)	6.755
	b_t (J/mol)	101.998
	R^2	0.9449
D-R isotherm	q_m (mg/g)	99.269
	K (mol^2/kJ^2)	2.72 × 10^{-7}
	E (kJ/mol)	1.354
	R^2	0.9447

PFOA: Perfluorooctanoic acid; ChCl-HC: ChCl-modified hydrochar; R^2: coefficient of determination; D-R: Dubinin-Radushkevich.

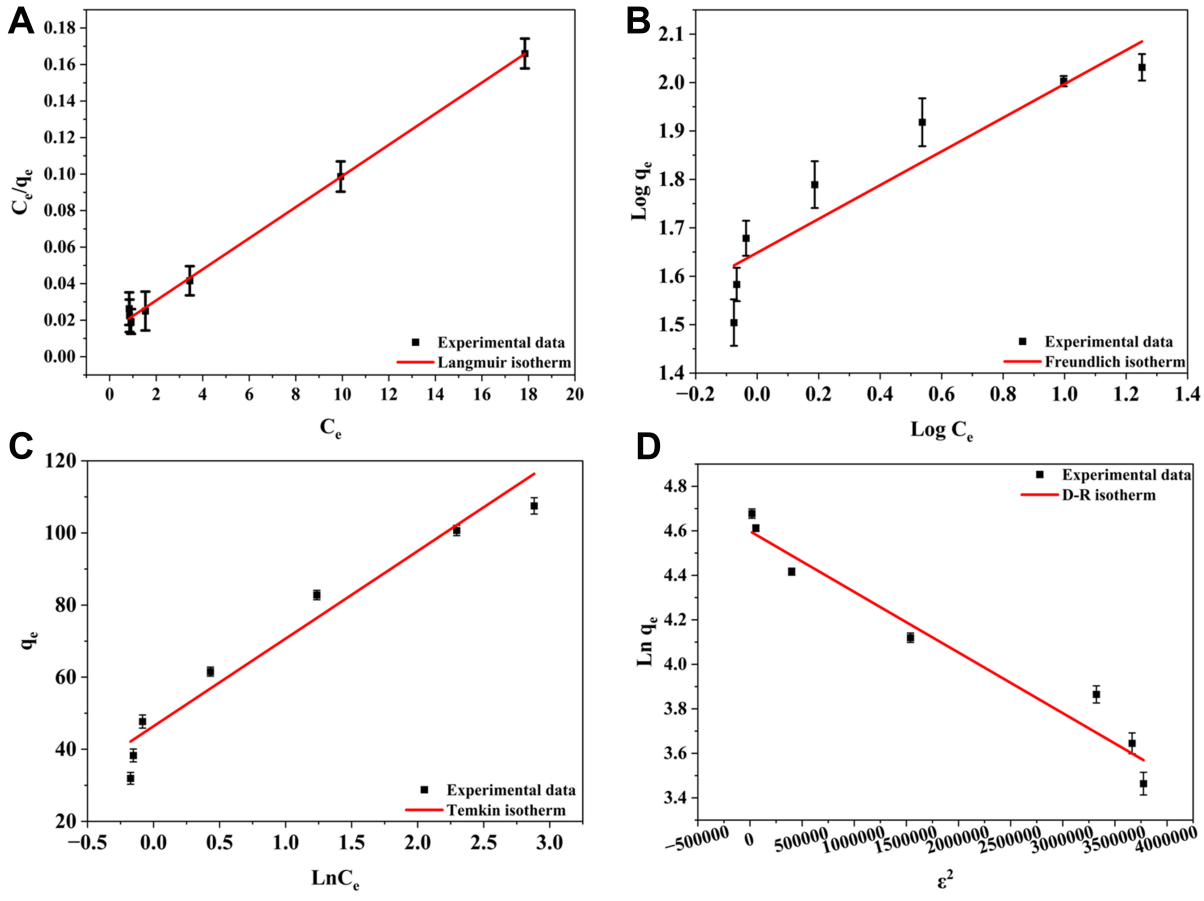


Figure 5. Linear adsorption isotherm plots of (A) Langmuir, (B) Freundlich, (C) Temkin, and (D) D-R model. D-R: Dubinin-Radushkevich.

second-order [Figure 6B], Elovich [Figure 6C], and intra-particle diffusion [Figure 6D] models, with the corresponding parameter values summarized in Table 4. Among these, the pseudo-second-order model exhibited the best fit as reflected by the highest correlation coefficient (R^2 = 0.9974), followed by Elovich (R^2

Table 4. Kinetic model parameters for PFOA adsorption onto 0.1 M ChCl-HC

Kinetic models		Parameters	Values
Pseudo-first-order		k_1 (min^{-1})	0.0408
		R^2	0.9614
Pseudo-second-order		k_2 ($g \cdot mg^{-1} \cdot min^{-1}$)	9.91×10^{-4}
		R^2	0.9974
Elovich model		α ($mg \cdot g^{-1} \cdot min^{-1}$)	5.6289
		β ($g \cdot mg^{-1}$)	0.1001
		R^2	0.9702
Intra-particle diffusion	Stage - I	k_{dI} ($mg/g/min^{0.5}$)	4.3084
		C_I (mg/g)	3.0035
		R_I^2	0.9388
	Stage - II	k_{dII} ($mg/g/min^{0.5}$)	0.0384
		C_{II} (mg/g)	47.2841
		R_{II}^2	0.9785

PFOA: Perfluorooctanoic acid; ChCl-HC: ChCl-modified hydrochar; R^2: coefficient of determination.

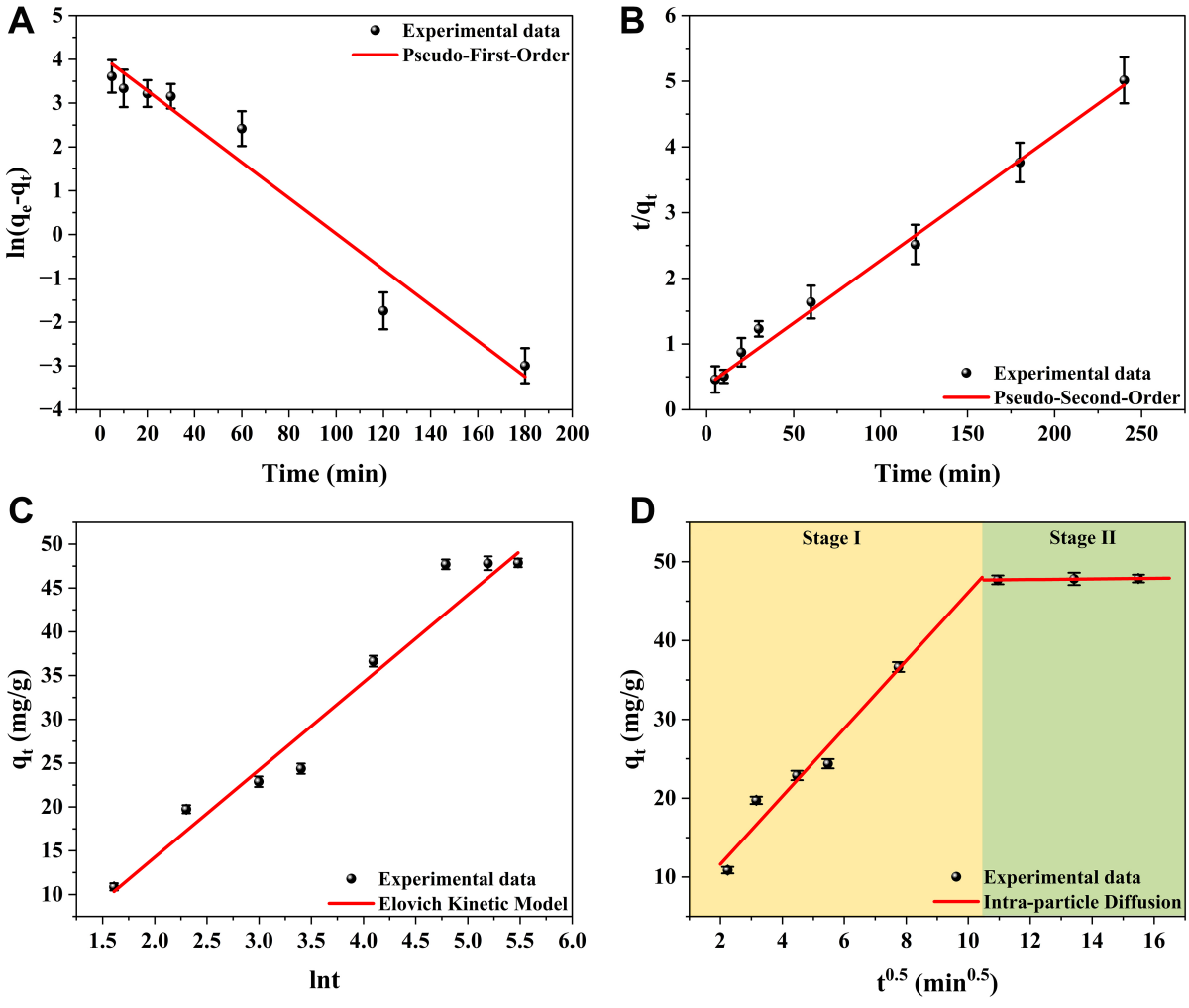


Figure 6. Linear adsorption kinetics plots of (A) pseudo-first-order, (B) pseudo-second-order, (C) Elovich, and (D) intra-particle diffusion model.

= 0.9702) and the pseudo-first-order (R^2 = 0.9614) models. Further, the intra-particle diffusion model was assessed by plotting q_t *vs.* $t^{0.5}$, as shown in Figure 6D. Two linear stages were observed: an initial rapid stage I (t ≤ 109 min) dominated by surface diffusion, and a slower subsequent stage II (109 min < t < 240 min), approaching equilibrium, governed by the intra-particle diffusion process[56]. The decrease in the rate constant k_{d1} to k_{d2} indicates reduced site availability and concentration gradient over time, while the increase in C_1 to C_2 suggests thicker boundary layer formation and lower external mass transfer[57]. As the q_t *vs.* $t^{0.5}$ plot did not pass through the origin, adsorption was controlled by both intra-particle and film diffusion, with film diffusion being the dominant mechanism.

Effect of humic acid and bridging ion

The adsorption of PFOA by 0.1 M ChCl-HC was evaluated in the presence of humic acid, as a representative of organic matter. The increase in the concentration of humic acid leads to the continuous decrease of PFOA adsorption [Figure 7A]. The presence of humic acid, which also bears a negative charge, leads to competition with PFOA for the adsorption sites on the adsorbent surface[51]. The effect of bridging ion on PFOA adsorption on the 0.1 M ChCl-HC was examined using varying concentrations of $CaCl_2$ (5-50 mM). The presence of Ca^{2+} enhanced PFOA adsorption at the lower concentration, primarily due to electrostatic interactions and the bridging effect between the adsorbent surface and PFOA molecules. However, beyond 20 mM $CaCl_2$, removal efficiency declined [Supplementary Figure 4A]. This reduction can be attributed to electrical double-layer compression, which diminishes electrostatic attraction, and the competitive interaction of chloride ions with adsorption sites[51,58,59]. The control study showed an increasing trend in the removal efficiency of PFOA [Supplementary Figure 4B]. These observations highlight the concentration-dependent dual role of $CaCl_2$, reinforcing the importance of ionic strength and electrolyte composition in regulating PFOA adsorption behavior.

Regeneration and comparative evaluation

Regeneration is essential for ensuring the economic and practical feasibility of any adsorbent material. In this study, the reusability of 0.1 M ChCl-HC was assessed over five adsorption-desorption cycles. The adsorption of PFOA on the 0.1 M ChCl-HC decreases with an increase in the number of cycles [Figure 7B]. A progressive decline in performance was observed, with PFOA removal efficiency dropping to 48.47% and adsorption capacity to 24.23 mg/g by the fifth cycle, likely due to residual PFOA molecules remaining on the adsorbent surface.

Table 5 presents a comparative evaluation of different adsorbents for PFOA removal, detailing their surface area, operational parameters, removal efficiencies, adsorption kinetics, and regeneration performance[60-63]. Among the tested materials, the 0.1 M ChCl-HC synthesized in this study demonstrated the highest surface area and achieved rapid and effective PFOA removal, reaching 95.4% in 2 h. The adsorption process followed pseudo-second-order kinetics with R^2 = 0.997. and the adsorbent retained its performance over five regeneration cycles. Overall, the developed material outperforms many previously reported adsorbents, including various nanocomposites, graphene oxide, biochar, and unmodified hydrochar.

Furthermore, based on economic analysis, commercial activated carbon with an adsorption capacity of 190.54 μmol/g[64] can remove approximately 0.0789 kg of PFOA per kg of adsorbent. Considering its market price of $11.2/kg[65]. This translates to an estimated treatment cost of about $142/kg of PFOA removed. In contrast, this study exhibits an adsorption capacity of 72.62 mg/g, equivalent to 0.0726 kg of PFOA removed per kg of 0.1 M ChCl-HC. Saba *et al.* estimated the cost of hydrochar to be $117.24/ton[66]. Based on this value and including the costs of other chemicals used for modification, the total cost of PFOA removal was

Table 5. Comparison of other adsorbents with 0.1 M ChCl-HC for the removal of PFOA

Adsorbents	Surface area (m^2/g)	Concentration	Dose (mg/L)	T (h)	Removal efficiency (%)	Kinetics	Regeneration cycle	Ref.
ZnO-Ag-$ZnAl_2O_4$	32.4	100 mg/L	300	4	93.1	PFO (R^2: 0.985)	-	[60]
GO-PEI	7.96	50 mg/L	1,000	15	94.1	PSO (R^2: 0.978)	5	[61]
Polyethyleneimine-modified biochar	0.131	0.121 mmol/L	150	20	95	PSO (R^2: 0.984)	4	[62]
Hydrochar	-	800 $ng{\cdot}L^{-1}$	5,000	1	0-20	PSO (R^2: 0.781-0.916)	-	[63]
0.1 M ChCl-HC	62.188	20 mg/L	400	2	95.4	PSO (R^2: 0.997)	5	This study

ChCl-HC: ChCl-modified hydrochar; PFOA: perfluorooctanoic acid; PFO: pseudo-first-order; R^2: coefficient of determination; GO-PEI: polyethyleneimine modified graphene oxide; PSO: pseudo-second-order.

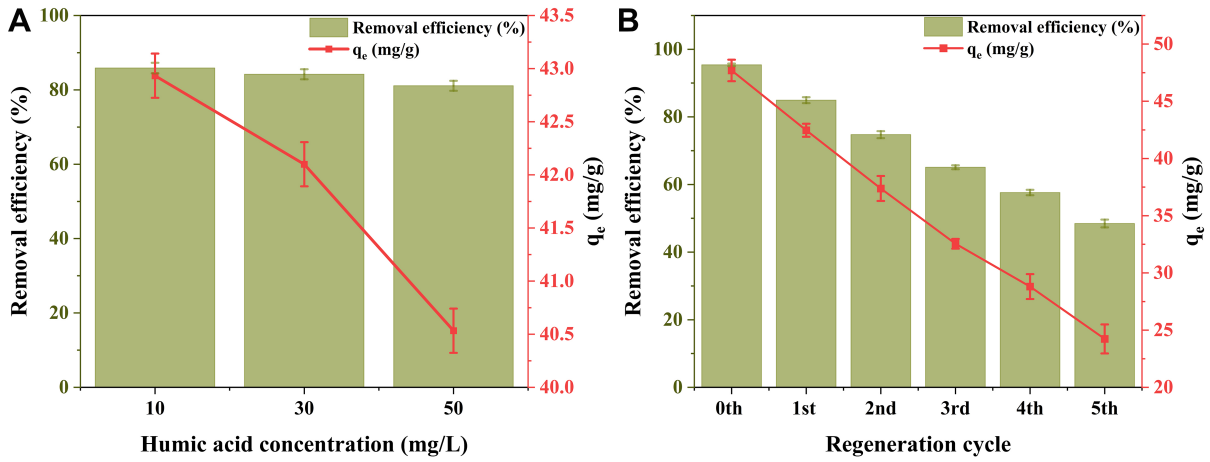


Figure 7. (A) Effect of humic acid on PFOA adsorption on 0.1 M ChCl-HC; (B) Regeneration study using 50% ethanol (Experimental conditions: PFOA concentration: 20 mg/L, Adsorbent dose: 400 mg/L, $CaCl_2$: 20 mM, Temperature: 298 K, and RPM: 250). PFOA: Perfluorooctanoic acid; ChCl-HC: ChCl-modified hydrochar; RPM: revolutions per minute.

calculated to be approximately $29.7/kg of PFOA. These findings indicated that, although commercial activated carbon demonstrated a higher adsorption capacity on a per-gram basis, hydrochar offers a more cost-effective solution for large-scale PFOA removal. The development of 0.1 M ChCl-HC represents a significant step forward in the quest for effective and sustainable water treatment technologies.

Adsorption mechanisms

The adsorption of PFOA onto 0.1 M ChCl-HC was primarily driven by physisorption, as indicated by the isotherm analysis. The anionic and hydrophobic nature of PFOA facilitated adsorption through multiple pathways. At the experimental pH of ~4.4, below the pH_{zpc} of 4.9, the positively charged surface of 0.1 M ChCl-HC promoted electrostatic attraction with PFOA, and the addition of divalent Ca^{2+} ions further enhanced adsorption through bridging interactions[30,51,67]. The perfluorinated tail of PFOA, composed of a long chain of C–F bonds, is highly hydrophobic[67], which could interact with the hydrophobic region of the 0.1 M ChCl-HC, leading to the hydrophobic interaction. Additionally, the appearance of new peaks and observed shift in the FTIR spectra after adsorption, as discussed in section "FTIR analysis" [Figure 2A], provided evidence for electrostatic interaction and hydrogen bonding between PFOA and the adsorbent. Overall, these findings demonstrate that a combination of electrostatic attraction, hydrophobic interaction, and hydrogen bonding governs the adsorption of PFOA.

CONCLUSIONS

This study demonstrates the potential of HTC for valorizing the potato peel waste into hydrochar and its subsequent application as an effective adsorbent for environmental remediation. Among the hydrochars synthesized under different operating conditions, the maximum surface area (28.055 m^2/g) was observed for the hydrochar produced at 180 °C for 4 h. Upon further modification with 0.1 M ChCl, the surface area significantly increased to 62.188 m^2/g, indicating improvement in surface activity and adsorption potential. The feasibility study was conducted using 0.1 M ChCl-HC for the removal of PFOA from aqueous matrices. The addition of calcium chloride notably improved the adsorption performance, increasing PFOA removal efficiency from 35.6% to 95.4% primarily due to the divalent bridging effect of Ca^{2+} ions, which strengthened the electrostatic interaction between PFOA and the adsorbent surface. The adsorption behavior was best described by the Langmuir isotherm and the pseudo-second-order kinetic model, while the underlying mechanism primarily involved electrostatic interactions, hydrogen bonding, and hydrophobic interactions. Overall, this study highlights the potential of ChCl-HC, in combination with $CaCl_2$ as a bridging agent, as a sustainable and efficient solution for the removal of PFOA from aqueous matrices.

DECLARATIONS

Authors' contributions

Investigation, data curation, visualization, writing - original draft: Sinha, S.
Investigation, visualization, writing - original draft: Mahanty, B.
Conceptualization, methodology, resources, supervision, writing - review and editing: Hait, S.

Availability of data and materials

Data and materials are available from the corresponding authors upon reasonable request.

Financial support and sponsorship

The fellowship grant awarded to Sinha, S. [IF210600] by the Department of Science and Technology, Government of India, is gratefully acknowledged.

Conflicts of interest

All authors declared that there are no conflicts of interest.

Ethical approval and consent to participate

Not applicable.

Consent for publication

Not applicable.

Copyright

© The Author(s) 2025.

REFERENCES

1. Singh, S. V.; Singh, K.; Kumar, N. Sustainable food waste utilization in the context of the Indian hospitality industry. In *Promoting sustainable gastronomy tourism and community development*. IGI Global; 2024. pp. 229-41. DOI
2. Swati, A.; Hait, S. Greenhouse gas emission during composting and vermicomposting of organic wastes - a review. *CLEAN. Soil. Air. Water.* **2018**, *46*, 1700042. DOI
3. UN Environment Programme. Solid waste management. https://www.unep.org/explore-topics/resource-efficiency/what-we-do/cities/solid-waste-management. (accessed 2025-10-29).

4. Khanal, S.; Karimi, K.; Majumdar, S.; et al. Sustainable utilization and valorization of potato waste: state of the art, challenges, and perspectives. *Biomass. Conv. Bioref.* **2024**, *14*, 23335-60. DOI
5. Vescovo, D.; Manetti, C.; Ruggieri, R.; et al. The valorization of potato peels as a functional ingredient in the food industry: a comprehensive review. *Foods* **2025**, *14*, 1333. DOI PubMed PMC
6. Amenyeku, G.; Cobbina, S. J.; Asare, W.; Teye, G. K. Hydrothermal carbonization of organic waste using faecal sludge as a water source: response surface methodology-Box Behnken design. *Environ. Challenges.* **2024**, *15*, 100900. DOI
7. Mahata, S.; Periyavaram, S. R.; Akkupalli, N. K.; Srivastava, S.; Matli, C. A review on co-hydrothermal carbonization of sludge: effect of process parameters, reaction pathway, and pollutant transport. *J. Energy. Inst.* **2023**, *110*, 101340. DOI
8. Basso, D.; Patuzzi, F.; Castello, D.; et al. Agro-industrial waste to solid biofuel through hydrothermal carbonization. *Waste. Manag.* **2016**, *47*, 114-21. DOI
9. Li, L.; Diederick, R.; Flora, J. R.; Berge, N. D. Hydrothermal carbonization of food waste and associated packaging materials for energy source generation. *Waste. Manag.* **2013**, *33*, 2478-92. DOI PubMed
10. Niinipuu, M.; Latham, K. G.; Boily, J. F.; Bergknut, M.; Jansson, S. The impact of hydrothermal carbonization on the surface functionalities of wet waste materials for water treatment applications. *Environ. Sci. Pollut. Res. Int.* **2020**, *27*, 24369-79. DOI PubMed PMC
11. Fang, J.; Gao, B.; Chen, J.; Zimmerman, A. R. Hydrochars derived from plant biomass under various conditions: characterization and potential applications and impacts. *Chem. Eng. J.* **2015**, *267*, 253-9. DOI
12. Czerwińska, K.; Śliz, M.; Wilk, M. Hydrothermal carbonization process: fundamentals, main parameter characteristics and possible applications including an effective method of SARS-CoV-2 mitigation in sewage sludge. A review. *Renew. Sustain. Energy. Rev.* **2022**, *154*, 111873. DOI
13. Kozyatnyk, I.; Benavente, V.; Weidemann, E.; Gentili, F. G.; Jansson, S. Influence of hydrothermal carbonization conditions on the porosity, functionality, and sorption properties of microalgae hydrochars. *Sci. Rep.* **2023**, *13*, 8562. DOI PubMed PMC
14. Goyi, A. A.; Sher Mohammad, N. M.; Omer, K. M. Nitrogen-rich, potato peel-derived hydrochar as an effective dye adsorbent. *Biofuels* **2024**, *15*, 1131-44. DOI
15. Xiao, K.; Liu, H.; Li, Y.; et al. Correlations between hydrochar properties and chemical constitution of orange peel waste during hydrothermal carbonization. *Bioresour. Technol.* **2018**, *265*, 432-6. DOI PubMed
16. Monlau, F.; Sambusiti, C.; Antoniou, N.; Zabaniotou, A.; Solhy, A.; Barakat, A. Pyrochars from bioenergy residue as novel bio-adsorbents for lignocellulosic hydrolysate detoxification. *Bioresour. Technol.* **2015**, *187*, 379-86. DOI PubMed
17. Sun, T.; Wang, F.; Xie, Y.; et al. Biochar remediation of PFOA contaminated soil decreased the microbial network complexity. *J. Environ. Chem. Eng.* **2023**, *11*, 109239. DOI
18. Xu, M.; Cui, Z.; Zhao, L.; Hu, S.; Zong, W.; Liu, R. Characterizing the binding interactions of PFOA and PFOS with catalase at the molecular level. *Chemosphere* **2018**, *203*, 360-7. DOI PubMed
19. Zhang, D. Q.; Zhang, W. L.; Liang, Y. N. Adsorption of perfluoroalkyl and polyfluoroalkyl substances (PFASs) from aqueous solution - a review. *Sci. Total. Environ.* **2019**, *694*, 133606. DOI PubMed
20. Guo, R.; Liu, X.; Liu, J.; et al. Occurrence, partition and environmental risk assessment of per- and polyfluoroalkyl substances in water and sediment from the Baiyangdian Lake, China. *Sci. Rep.* **2020**, *10*, 4691. DOI PubMed PMC
21. Miserli, K.; Boti, V.; Konstantinou, I. Analysis of perfluorinated compounds in sewage sludge and hydrochar by UHPLC LTQ/Orbitrap MS and removal assessment during hydrothermal carbonization treatment. *Sci. Total. Environ.* **2024**, *929*, 172650. DOI PubMed
22. Araújo, R. G.; Rodríguez-Hernandéz, J. A.; González-González, R. B.; et al. Detection and tertiary treatment technologies of poly-and perfluoroalkyl substances in wastewater treatment plants. *Front. Environ. Sci.* **2022**, *10*, 864894. DOI
23. Miserli, K.; Athanasiou, V.; Boti, V.; Hela, D.; Konstantinou, I. Determination of PFAS in wastewaters and natural waters by solid phase extraction and UHPLC LTQ/Orbitrap MS for assessing occurrence and removals. *Case. Stud. Chem. Environm. Eng.* **2023**, *8*, 100505. DOI
24. Afrooz, M.; Zeynali, R.; Soltan, J.; Mcphedran, K. N. A novel biochar adsorbent for treatment of perfluorooctanoic acid (PFOA) contaminated water: exploring batch and dynamic adsorption behavior. *J. Water. Process. Eng.* **2025**, *69*, 106586. DOI
25. United States Environmental Protection Agency. Per- and polyfluoroalkyl substances (PFAS). Final PFAS National Primary Drinking Water Regulation. 2025. https://www.epa.gov/sdwa/and-polyfluoroalkyl-substances-pfas. (accessed 2025-10-29).
26. Liu, F.; Pignatello, J. J.; Sun, R.; Guan, X.; Xiao, F. A comprehensive review of novel adsorbents for per- and polyfluoroalkyl substances in water. *ACS. EST. Water.* **2024**, *4*, 1191-205. DOI
27. Chen, F.; Chen, J.; Liu, X.; et al. Removal of per- and polyfluoroalkyl substances by activated hydrochar derived from food waste: sorption performance and desorption hysteresis. *Environ. Pollut.* **2023**, 122820. DOI
28. Buarque, F. S.; Monteiro E Silva, S. A.; Ribeiro, B. D. Choline chloride-based deep eutectic solvent as an inhibitor of metalloproteases (collagenase and elastase) in cosmetic formulation. *3. Biotech.* **2023**, *13*, 219. DOI PubMed PMC
29. Huang, J.; Cao, S.; Liu, Z.; Tian, J.; Xi, C.; Chen, Z. High-efficiency removal of methcathinone from water using a novel DES modified magnetic biochar nanocomposite. *J. Environ. Chem. Eng.* **2022**, *10*, 108456. DOI
30. Xu, J.; Liu, Z.; Zhao, D.; Gao, N.; Fu, X. Enhanced adsorption of perfluorooctanoic acid (PFOA) from water by granular activated carbon supported magnetite nanoparticles. *Sci. Total. Environ.* **2020**, *723*, 137757. DOI PubMed
31. Hassan, M.; Du, J.; Liu, Y.; et al. Magnetic biochar for removal of perfluorooctane sulphonate (PFOS): interfacial interaction and

adsorption mechanism. *Environ. Technol. Innov.* **2022**, *28*, 102593. DOI

32. García-Suárez, E. J.; Menéndez-Vázquez, C.; García, A. B. Chemical stability of choline-based ionic liquids supported on carbon materials. *J. Mol. Liq.* **2012**, *169*, 37-42. DOI
33. Kalam, S.; Abu-Khamsin, S. A.; Kamal, M. S.; Patil, S. Surfactant adsorption isotherms: a review. *ACS. Omega.* **2021**, *6*, 32342-8. DOI PubMed PMC
34. Boparai, H. K.; Joseph, M.; O'Carroll, D. M. Kinetics and thermodynamics of cadmium ion removal by adsorption onto nano zerovalent iron particles. *J. Hazard. Mater.* **2011**, *186*, 458-65. DOI PubMed
35. Niaz, W.; Zhang, D.; Ahmad, Z.; et al. Efficient removal of perfluorooctanoic acid (PFOA) and perfluorooctane sulfonic acid (PFOS) from aqueous solution using modified biochar: preparation, performance, and mechanistic insights. *J. Environ. Chem. Eng.* **2024**, *12*, 114894. DOI
36. Angı, A.; Sanlı, D.; Erkey, C.; Birer, Ö. Catalytic activity of copper (II) oxide prepared via ultrasound assisted Fenton-like reaction. *Ultrason. Sonochem.* **2014**, *21*, 854-9. DOI PubMed
37. Robertson, M.; Lamb, B.; Griffin, A.; He, L.; Ma, B.; Qiang, Z. Critical role of pore size on perfluorooctanoic acid adsorption behaviors in carbonaceous sorbents. *Mater. Horiz.* **2025**, *12*, 2935-44. DOI PubMed
38. Barmina, I.; Lickrastina, A.; Zake, M.; Arshanitsa, A.; Solodovnik, V.; Telysheva, G. Experimental study of thermal decomposition and combustion of lignocellulosic biomass pellets. *Latv. J. Phys. Tech. Sci.* **2013**, *50*, 35-48. DOI
39. Li, P.; Wang, Y.; Hou, Q.; et al. Preparation of cellulose nanofibrils from okara by high pressure homogenization method using deep eutectic solvents. *Cellulose* **2020**, *27*, 2511-20. DOI
40. Khan, Z.; Yusup, S.; Ahmad, M. M. Thermogravimetric analysis of palm oil wastes decomposition. In *2011 IEEE Conference on Clean Energy and Technology (CET)*, Kuala Lumpur, Malaysia. June 27-29, 2011. IEEE; 2011. pp. 205-8. DOI
41. Adebisi, G. A.; Chowdhury, Z. Z.; Abd Hamid, S. B.; Ali, E. Hydrothermally treated banana empty fruit bunch fiber activated carbon for Pb(II) and Zn(II) removal. *BioResources* **2016**, *11*, 9686-709. DOI
42. Goyi, A. A.; Sher Mohammad, N. M.; Omer, K. M. Preparation and characterization of potato peel derived hydrochar and its application for removal of Congo red: a comparative study with potato peel powder. *Int. J. Environ. Sci. Technol.* **2024**, *21*, 631-42. DOI
43. Sevilla, M.; Fuertes, A. The production of carbon materials by hydrothermal carbonization of cellulose. *Carbon* **2009**, *47*, 2281-9. DOI
44. Mukti, N. I. F.; Ariyanto, T.; Sediawan, W. B.; Prasetyo, I. Efficacy of modified carbon molecular sieve with iron oxides or choline chloride-based deep eutectic solvent for the separation of CO_2/CH_4. *RSC. Adv.* **2023**, *13*, 23158-68. DOI PubMed PMC
45. Gao, P.; Zhou, Y.; Meng, F.; et al. Preparation and characterization of hydrochar from waste eucalyptus bark by hydrothermal carbonization. *Energy* **2016**, *97*, 238-45. DOI
46. Liang, M.; Zhang, K.; Lei, P.; Wang, B.; Shu, C.; Li, B. Fuel properties and combustion kinetics of hydrochar derived from co-hydrothermal carbonization of tobacco residues and graphene oxide. *Biomass. Conv. Bioref.* **2020**, *10*, 189-201. DOI
47. Prasannamedha, G.; Kumar, P. S.; Kyzas, G. Hydrothermal carbonization of waste sugarcane bagasse for the effective removal of emerging contaminants from aqueous solution. *Adsorpt. Sci. Technol.* **2022**, *2022*, 8684737. DOI
48. Liu, P.; Hao, J.; Liang, S.; Liang, G.; Wang, J.; Zhang, Z. Choline chloride and itaconic acid-based deep eutectic solvent as an efficient and reusable medium for the preparation of 13-aryl-5H-dibenzo[b,i]xanthene-5,7,12,14(13H)-tetraones. *Monatsh. Chem.* **2016**, *147*, 801-8. DOI
49. Potchamyou Ngatcha, A. D.; Zhao, A.; Zhang, S.; et al. Determination of active sites on the synthesis of novel Lewis acidic deep eutectic solvent catalysts and kinetic studies in microalgal biodiesel production. *RSC. Adv.* **2023**, *13*, 10110-22. DOI PubMed PMC
50. Pervez, M. N.; Jiang, T.; Mahato, J. K.; et al. Surface modification of graphene oxide for fast removal of per- and polyfluoroalkyl substances (PFAS) mixtures from river water. *ACS. ES. T. Water.* **2024**, *4*, 2968-80. DOI PubMed PMC
51. Lei, X.; Yao, L.; Lian, Q.; et al. Enhanced adsorption of perfluorooctanoate (PFOA) onto low oxygen content ordered mesoporous carbon (OMC): adsorption behaviors and mechanisms. *J. Hazard. Mater.* **2022**, *421*, 126810. DOI PubMed
52. Yu, Q.; Zhang, R.; Deng, S.; Huang, J.; Yu, G. Sorption of perfluorooctane sulfonate and perfluorooctanoate on activated carbons and resin: kinetic and isotherm study. *Water. Res.* **2009**, *43*, 1150-8. DOI PubMed
53. Yan, Z.; Sun, Y.; Yan, J.; Liu, R.; Zhang, J.; Song, J. Rapid adsorption of per- and polyfluoroalkyl substances (PFAS) on N-doped porous carbons (NPCs) derived from ZIF-8 over a wide pH range: adsorption behaviors and mechanisms. *Sep. Purif. Technol.* **2025**, *365*, 132575. DOI
54. Kasalica, K.; Petronijevic, N.; Radulovic, J.; et al. Adsorption analysis of PFOA on activated carbon and ion-exchange resin: a comparative study using four isotherm models. *J. Serb. Chem. Soc.* **2024**, *89*, 1619-28. DOI
55. Tian, D.; Geng, D.; Tyler Mehler, W.; et al. Removal of perfluorooctanoic acid (PFOA) from aqueous solution by amino-functionalized graphene oxide (AGO) aerogels: influencing factors, kinetics, isotherms, and thermodynamic studies. *Sci. Total. Environ.* **2021**, *783*, 147041. DOI PubMed
56. Sahu, S.; Yadav, M. K.; Gupta, A. K.; et al. Modeling defluoridation of real-life groundwater by a green adsorbent aluminum/olivine composite: isotherm, kinetics, thermodynamics and novel framework based on artificial neural network and support vector machine. *J. Environ. Manage.* **2022**, *302*, 113965. DOI PubMed
57. Ghaedi, M.; Shokrollahi, A.; Hossainian, H.; Kokhdan, S. N. Comparison of activated carbon and multiwalled carbon nanotubes for efficient removal of eriochrome cyanine R (ECR): kinetic, isotherm, and thermodynamic study of the removal process. *J. Chem. Eng.*

Data. **2011**, *56*, 3227-35. DOI

58. Wang, F.; Liu, C.; Shih, K. Adsorption behavior of perfluorooctanesulfonate (PFOS) and perfluorooctanoate (PFOA) on boehmite. *Chemosphere* **2012**, *89*, 1009-14. DOI PubMed
59. Hakimabadi, S. G.; Taylor, A.; Pham, A. L. Factors affecting the adsorption of per- and polyfluoroalkyl substances (PFAS) by colloidal activated carbon. *Water. Res.* **2023**, *242*, 120212. DOI PubMed
60. Yang, H.; Joe, H. J.; Park, S.; Kim, S. K.; Lee, C. Enhanced removal of perfluorooctanoic acid (PFOA) from water using ZnO-Ag-$ZnAl_2O_4$ composites: performance and mechanistic insights. *J. Water. Process. Eng.* **2024**, *61*, 105288. DOI
61. Lei, X.; Lian, Q.; Zhang, X.; et al. Removal of perfluorooctanoic acid via polyethyleneimine modified graphene oxide: effects of water matrices and understanding mechanisms. *Chemosphere* **2022**, *308*, 136379. DOI PubMed
62. Imran, A.; Lei, X.; Shoemaker, D. J.; et al. Adsorption of PFCAs using polyethyleneimine modified Biochar: role of chain length and effects of water matrices. *Chemosphere* **2025**, *386*, 144650. DOI PubMed
63. Niinipuu, M.; Bergknut, M.; Boily, J. F.; Rosenbaum, E.; Jansson, S. Influence of water matrix and hydrochar properties on removal of organic and inorganic contaminants. *Environ. Sci. Pollut. Res. Int.* **2020**, *27*, 30333-41. DOI PubMed PMC
64. Fagbayigbo, B. O.; Opeolu, B. O.; Fatoki, O. S.; Akenga, T. A.; Olatunji, O. S. Removal of PFOA and PFOS from aqueous solutions using activated carbon produced from Vitis vinifera leaf litter. *Environ. Sci. Pollut. Res. Int.* **2017**, *24*, 13107-20. DOI PubMed
65. Wu, Y.; Qi, L.; Chen, G. A mechanical investigation of perfluorooctane acid adsorption by engineered biochar. *J. Clean. Prod.* **2022**, *340*, 130742. DOI
66. Saba, A.; Mcgaughy, K.; Reza, M. Techno-economic assessment of co-hydrothermal carbonization of a coal-miscanthus blend. *Energies* **2019**, *12*, 630. DOI
67. Du, Z.; Deng, S.; Bei, Y.; et al. Adsorption behavior and mechanism of perfluorinated compounds on various adsorbents - a review. *J. Hazard. Mater.* **2014**, *274*, 443-54. DOI PubMed
68. Mahanty, B.; Mondal, S. Synthesis of magnetic biochar using agricultural waste for the separation of Cr(VI) from aqueous solution. *Arab. J. Sci. Eng.* **2021**, *46*, 10803-18. DOI